Radiative nucleon capture with quasi-separable potentials

Shubhchintak[1,5], C A Bertulani[1,2], A M Mukhamedzhanov[3] and A T Kruppa[4]

[1] Department of Physics and Astronomy, Texas A&M University-Commerce, Commerce, TX 75429, USA
[2] Department of Physics and Astronomy, Texas A&M University, College Station, Texas 77843, USA
[3] Cyclotron Institute, Texas A&M University, College Station, TX 77843, USA
[4] Institute for Nuclear Research, Hungarian Academy of Sciences, Debrecen, PO Box 51, H-4001, Hungary

E-mail: shub.shubhchintak@tamuc.edu, carlos.bertulani@tamuc.edu, akram@comp.tamu.edu and atk@atomki.mta.hu

Abstract

We study radiative capture reactions using quasi-separable potentials. This procedure allows an easier treatment of non-local effects that can be extended to three-body problems. Using this technique, we calculate the neutron and proton radiative capture cross sections on ^{12}C. The results obtained are shown to be in good agreement with the available experimental data.

Keywords: radiative proton capture, radiative neutron capture, separable potentials, elastic scattering

(Some figures may appear in colour only in the online journal)

1. Introduction

Separable potentials have been widely used in the literature to study nucleon–nucleon as well as nucleon-nucleus scattering problems [1–7]. Short range nuclear interactions by nature are non-local and can be treated in separable forms However, this non-locality is often weak and therefore equivalent local potentials, e.g., of Woods–Saxon (WS) type, can be used to replace non-local potentials to a good extent [8]. Although separable potentials have found extensive use in nuclear physics, they have also been used in other branches of physics. In nuclear

---

[5] Author to whom all correspondence should be addressed.

physics their main application is in the realm of three or few-body scattering problems [9, 10], where local potentials increase computational efforts. Actually, in three-body problems one has to find the 'off-energy-shell' scattering amplitude, which can be handled more easily and in a more transparent manner, with separable potentials. Separable potentials help to convert the three-body into effective two-body problems [10], thus simplifying the problem.

Our interest in this work is to invoke separable potentials to calculate cross sections for direct radiative nucleon capture reactions of importance for nuclear astrophysics. We make use of experimental phase shifts obtained from nucleon-nucleus scattering considering non-local potentials of separable form. We will closely follow the quasi-separable potential technique developed in [5, 6]. In the literature there are a large number of separable potentials available which have been proven to work very well in different energy ranges. We refer to at least three of these given in [5–7, 10]. The first potential set given in [5, 6] explains very well nucleon+^{12}C experimental phase shifts for $L \leqslant 2$ in the low energy range (below $\sim$5–7 MeV), whereas the second potential set of [7] yields good agreement with experiments at higher energies. The third set, used in [10], is constructed in such a way so as to improve shortcomings observed in the first two sets to a satisfactory extent.

As we are interested in astrophysical reactions, which take place at low energies, the first set of potential is suitable for our purposes. Furthermore, the complication in the case of charge-particle scattering can be taken care of in a simple and accurate manner using this potential. The potential parameters required for proton-nucleus scattering are almost the same as those for neutron-nucleus scattering. Therefore, as an application of the method we calculate direct neutron and proton capture cross sections for ^{12}C(n, γ)^{13}C and ^{12}C(p, γ)^{13}N reactions.

The nuclei under interest, ^{13}C and ^{13}N are very important in astrophysical scenarios. They are formed in the CNO cycle, where a proton capture on ^{12}C (following the triple-α process) leads to ^{13}N, which then decays by positron emission and forms ^{13}C [11, 12]. This is also known as the cold CNO cycle and takes place in massive main-sequence stars in the reaction chain ^{12}C(p, γ)^{13}N(β^{+}, ν)^{13}C(p, γ)^{14}N(p, γ)^{15}O(β^{+}, ν)^{15}N(p, α) ^{12}C. However, in high temperature conditions occurring in novae and x-ray bursts, the ^{13}N formed after the first step undergoes proton capture and yields a new cycle, known as the hot CNO cycle ^{12}C(p, γ)^{13}N(p, γ)^{14}O(β^{+}, ν)^{14}N(p, γ)^{15}O(β^{+}, ν)^{15}N(p, α) ^{12}C. ^{13}C also leads to neutron formation and acts as a neutron source in helium burning asymptotic giant branch stars by means of the ^{13}C(α, n)^{16}O reaction [13]. In neutron rich environments, ^{12}C can also undergo neutron capture processes and start a neutron induced CNO cycle that leads to the formation of other heavier elements and hence a breakout of the CNO cycle.

Neutron capture cross sections on ^{12}C have been measured at thermal as well as at neutron energies between 10 and 550 MeV [14–17]. The cross section has contributions from four low-lying states of ^{13}C and deviates from the usual $1/v$ law [16]. Its energy dependence has been studied within different theoretical models [18–21] and it has been found that the capture is dominated by the transition to the first excited state (e.s.) of ^{13}C, which is a weakly bound halo state [22]. The ^{12}C(p,γ)^{13}N cross sections have also been measured at long energy interval 70–2500 keV [23–26] and are well explained theoretically using direct capture plus resonant contributions. In fact, many different direct capture models have been used to calculate the nucleon capture cross sections which differ in the way one chooses initial and final states. In this context, the present work adds an additional method to obtain the nucleon capture reactions. Such reactions are of enormous interest for nuclear astrophysics (see, e.g. [27]). As separable potentials are easier to handle non-local effects, they would enable improvements in numerical calculations of cross sections used to determine element production in several astrophysical scenarios involving both two-body and three-body reactions.

Another goal of this work is to test the behavior of the continuum wavefunction obtained with the adopted separable potential so as to use it in Faddeev-AGS equations for three-body systems.

This paper is organized in the following way. In section 2, we briefly describe our formalism to use non-local nucleon-nucleus potentials to obtain a feasible calculation of nucleon capture cross sections. In section 3, we present our results, including a phase-shift analysis to reproduce experimental results. Our conclusions are presented in section 4.

2. Formalism

2.1. Radiative capture in the potential model

For the direct radiative capture reaction $b + c \rightarrow a + \gamma$, where c is a nucleon, the cross section is given by (see, e.g., [28–30])

$$
\sigma_{\pi L}^{\mathrm{cap}} = \frac{(2\pi)^3}{k^2} \left(\frac{E_\gamma}{\hbar c}\right)^{2L+1} \frac{2(2I_a + 1)}{(2I_b + 1)(2I_c + 1)} \frac{L + 1}{L[(2L + 1)!!]^2}
$$
$$
\times \sum_{l,j,J} (2J + 1) \begin{Bmatrix} j & J & I_b \\ J_0 & j_0 & L \end{Bmatrix}^2 |\langle lj||O_{\pi L}||l_0 j_0\rangle|^2, \tag{1}
$$

where, πL stands for electric or magnetic transition of multipolarity L, and $E_\gamma = E_{\mathrm{c.m.}} + \epsilon$, with $E_{\mathrm{c.m.}}$ being the center of mass energy of the $b - c$ system with binding energy ϵ. k is the momentum corresponding to $E_{\mathrm{c.m.}}$ and I_a, I_b and I_c are the intrinsic spins of the respective particles.

Here, the relative angular momentum l of the pair $b - c$ couples with the spin of nucleon I_c to yield j, so that $\mathbf{l} + \mathbf{I}_c = \mathbf{j}$. This then couples with the intrinsic spin of the 'core' I_b to yield the initial total angular momentum $\mathbf{J} = \mathbf{j} + \mathbf{I}_b$. l_0, j_0 and J_0 denote the corresponding bound state quantum numbers. In equation (1), $\langle lj||O_{\pi L}||l_0 j_0\rangle$ is the reduced matrix element. For electric multipole transitions, which is the case of our interest, it is given by [28, 29] (see also equation A2.23 of [31])

$$
\langle lj||O_{\pi L}||l_0 j_0\rangle = \delta_{l+l_0+L,\mathrm{even}} (-1)^{(l_0+l-j+L-1/2)} \frac{e_L}{\sqrt{4\pi}} \sqrt{(2L + 1)(2j_0 + 1)}
$$
$$
\times \begin{pmatrix} j_0 & L & j \\ 1/2 & 0 & -1/2 \end{pmatrix} \int_0^\infty \mathrm{d}r r^L u_{l_0 j_0}^{J_0}(r) u_{lj}^J(r), \tag{2}
$$

where e_L is the effective charge given by $e_L = Z_b e (-m_c/m_a)^L + Z_c e (m_b/m_a)^L$, with m_i and Z_i being the masses and charges of the respective particles. $u_{l_0 j_0}^{J_0}(r)$ and $u_{lj}^J(r)$ are the bound state and continuum wavefunction, respectively.

Here, there is no advantage of using a separable potential and the bound state wavefunction can be calculated by solving the Schrödinger equation with a WS potential, where the potential depth is adjusted to get the corresponding binding energy of the state. We have verified this assertion by using the result of the potential model as described above, and compared to calculations for the bound state using the separable potential defined below using the code PSEUDO [32]. As shown, e.g., in [29], it is necessary to change the WS potential parameters to calculate the continuum wavefunctions and to reproduce in a reasonable fashion the experimental values of the radiative cross sections and astrophysical S-factors. Instead, here we calculate the continuum wavefunction to obtain the proper scattering matrix (S-matrix) for nucleon-nucleus scattering using the quasi-separable potential technique described

in [5, 6]. The advantage of the method is that it allows us a consistent reproduction of the experimental phase shifts and at the same time the radiative capture cross sections, using separable potentials for both situations. Moreover, separable potentials allow an easy implementation of three-body calculations which is our next goal. We will briefly discuss how to implement *S*-matrix calculations with this formalism for neutron-nucleus and proton-nucleus scattering.

2.2. S-matrices and wavefunctions from quasi-separable potentials

If we represent the initial state of the $b + c$ system in partial wave form as $|\alpha l j J M\rangle$, where α is the channel number representing the core state so that $I_\alpha = I_b$ (with the convention that $\alpha = 1$ represents the elastic channel) and l, j, J are the quantum numbers as explained above with M being the z-component of total angular momentum J, then the nuclear interaction in a quasi-separable form can be written as

$$V = - \sum_{\substack{\alpha l j, \beta l' j' \\ JM}} |\chi; \alpha l j J M\rangle \lambda^{J\Pi}_{\alpha l j, \beta l' j'} \langle \beta l' j' J M; \chi|, \tag{3}$$

where l', j', J' and M' are quantum numbers of the system in channel β. λ represents the coupling between the channels and the coupling matrix is considered to be symmetric i.e., $\lambda^{J\Pi}_{\alpha l j, \beta l' j'} = \lambda^{J\Pi}_{\beta l' j', \alpha l j}$. This assures that the potential is Hermitian and separability has been considered only in the relative motion variable r in each channel. $|\chi; \alpha l j J M\rangle$ denotes form factor vectors and in momentum space its representation is

$$\langle \alpha l j J M; k | \chi; \beta l' j' J' M' \rangle = \delta_{\alpha\beta} \delta_{ll'} \delta_{jj'} \delta_{JJ'} \delta_{MM'} i^{-l} u^J_{\alpha l j}(k),$$

where the form factor $u^J_{\alpha l j}(k)$, is given by

$$u^J_{\alpha l j}(k) = \sqrt{\frac{2}{\pi}} (2l)!! g^J_{\alpha l j}(k), \quad \text{with} \quad g^J_{\alpha l j}(k) = \frac{k^l}{[k^2 + (\beta^J_{\alpha l j})^2]^{(l+1)}}. \tag{4}$$

$\beta^J_{\alpha l j}$ is the fitting parameter having units of inverse length, with the assumption $\beta^J_{\alpha l j} = \beta_{l j}$.

One can write the *S*-matrix as

$$S^{J\Pi}_{\alpha l j, \beta l' j'} = \delta_{\alpha\beta} \delta_{ll'} \delta_{jj'} + i^{l'-l+1} \pi \mu k^{1/2}_\alpha u^J_{\alpha l j}(k_\alpha) \mathcal{T}^{J\Pi}_{\alpha l j, \beta l' j'} u^J_{\beta l' j'}(k_\beta) k^{1/2}_\beta, \tag{5}$$

where $\mathcal{T}^{J\Pi}_{\alpha l j, \beta l' j'}$ is a matrix related to *T*-matrix as

$$T^{J\Pi}_{\alpha l j, \beta l' j'}(k, k') = -i^{l'-l} u^J_{\alpha l j}(k) \mathcal{T}^{J\Pi}_{\alpha l j, \beta l' j'} u^J_{\beta l' j'}(k'), \tag{6}$$

satisfying the following coupled equation,

$$\mathcal{T}^{J\Pi}_{\alpha l j, \beta l' j'} = \lambda^{J\Pi}_{\alpha l j, \beta l' j'} - \sum_{\gamma l'' j''} \lambda^{J\Pi}_{\alpha l j, \gamma l'' j''} \mathcal{G}^{J\Pi}_{\gamma l'' j''} \mathcal{T}^{J\Pi}_{\gamma l'' j'', \beta l' j'}, \tag{7}$$

with

$$\mathcal{G}^{J\Pi}_{\gamma l'' j''} = \langle \gamma l'' j'' J M; \chi | G_0 | \chi; \gamma l'' j'' J M \rangle = \mu \int_0^\infty \frac{[u_{\gamma l'' j''}(k)]^2 k^2}{k^2_\gamma - k^2 + i\epsilon} dk. \tag{8}$$

In the above equation $G_0(z) = (z - H_0)^{-1}$ is the resolvent for unperturbed Hamiltonian H_0. Equation (5) is the *S*-matrix in a quasi-separable potential form for the case when c is a neutron and there is no Coulomb interaction. In the case of proton-nucleus scattering, one has to take care of the Coulomb potential V_c along with the nuclear potential V. The transition operator can be written as the sum of the pure Coulomb (*t*) and Coulomb modified nuclear (*τ*) transition operators, i.e $T = t + \tau$, where τ is given by

$$\tau = (1 + V_c G_c) T_c (1 + G_c V_c), \tag{9}$$

with $G_c(z) = (z - H_0 - V_c)^{-1}$ being the Coulomb-perturbed resolvent and T_c satisfies the equation $T_c = V + V G_c T_c$.

The reduced S-matrix expression in this case has a similar form as in equation (5), with all the quantities replaced by their Coulomb corrected form. That is,

$$S_{C,\alpha lj,\beta l'j'}^{J\Pi} = \delta_{\alpha\beta}\delta_{ll'}\delta_{jj'} + i^{l'-l+1}\pi\mu k_\alpha^{1/2} u_{C,\alpha lj}^J(k_\alpha) \mathcal{T}_{C,\alpha lj,\beta l'j'}^{J\Pi} u_{C,\beta l'j'}^J(k_\beta) k_\beta^{1/2}, \tag{10}$$

where the Coulomb corrected matrices, $\mathcal{T}_C$ and T_C satisfy a similar relation as in equation (6), i.e.,

$$T_{C,\alpha lj,\beta l'j'}^{J\Pi}(k, k') = -i^{l'-l} \, e^{i\sigma_l(k)} u_{C,\alpha lj}^J(k) \mathcal{T}_{C,\alpha lj,\beta l'j'}^{J\Pi} u_{C,\beta l'j'}^J(k') e^{i\sigma_{l'}(k')}. \tag{11}$$

In the above equation σ_l is the Coulomb phase shift and $u_{C,\alpha lj}^J(k)$ is the Coulomb corrected nuclear form factor given by,

$$u_{C,\alpha lj}^J(k) = \sqrt{\frac{2}{\pi}}\,(2l+1)!!\,C_l(\eta)g_{\alpha lj}^J(k)\exp\left[2\eta\arctan\left(\frac{k}{\beta_{\alpha lj}^J}\right)\right], \tag{12}$$

where η is the Coulomb parameter and the functions $C_l(\eta)$ are given by,

$$C_l(\eta) = \frac{\sqrt{l^2+\eta^2}}{l(2l+1)}\,C_{l-1}(\eta); \quad C_0(\eta) = \sqrt{\frac{2\pi\eta}{e^{2\pi\eta}-1}}. \tag{13}$$

For more detailed derivations of the quantities described above one is referred to [5, 6].

The elastic component of the S-matrix, i.e., $S_{1lj,1l'j'}^{J\Pi}$, is used to obtain the phase shifts δ_{lJ} which are related by $S = e^{2i\delta}$. Two steps are needed; the first one is to find the possible values of the parameters β and λ that reproduce all the resonances at right positions. These values are further improved by fitting to the experimental phase shifts. Once the potential parameters are all set, we solve the Schrödinger equation to obtain the scattering wavefunction which asymptotically behaves as,

$$u_{lj}^J(r)(r\to\infty) = -\sqrt{\frac{2}{\pi}}\,e^{i\delta_{lJ}}[F_l\cos(\delta_{lJ}) + G_l\sin(\delta_{lJ})], \tag{14}$$

where F_l and G_l are regular and irregular Coulomb wavefunctions.

3. Results and discussions

3.1. Phase-shifts

Neutron and proton radiative capture on ^{12}C lead to the formation of ^{13}C and ^{13}N, respectively. Given that the total neutron capture cross section has contributions from four low-lying states of ^{13}C [16], we calculate the neutron capture cross section to the states with spin parity $J^\pi = 1/2^-$ for the ground state, $1/2^+$ for the 1st e.s., $3/2^-$ for the 2nd e.s., and $5/2^+$ for the 3rd e.s., respectively. These states are formed by coupling of the 0^+ ground state of ^{12}C with the neutron in the $1p_{1/2}$, $2s_{1/2}$, $1p_{3/2}$ and $1d_{5/2}$ orbital with one neutron removal energy, S_n, equal to 4.95, 1.86, 1.27 and 1.09 MeV, respectively. The proton capture cross section on the other hand is only calculated for capture to the ground state of ^{13}N with $J^\pi = 1/2^-$, formed by coupling the $1p_{1/2}$ proton to the 0^+ ground state of ^{12}C, with a binding energy of $S_p = 1.94$ MeV. In order to calculate the bound state wavefunctions of ^{13}C, we use the WS parameters of [19], i.e., $r_0 = 1.236$ fm, $a = 0.62$ fm and $V_{so} = -7$ MeV. The values of the

Table 1. Fitting parameter β_{lj}. They are the same for both ^{13}C and ^{13}N.

| l	j	β_{lj} (fm^{-1})
0	1/2	0.57
1	1/2	1.76
1	3/2	1.22
2	3/2	2.16
2	5/2	2.96

Table 2. Strength parameter $\lambda^{J\pi}_{\alpha lj,\beta l'j'}$ used in equation (3), for ^{13}C and ^{13}N.

| Phase shift	$\alpha\ l\ j;\ \beta\ l'\ j'$	^{13}C	^{13}N
		$\lambda^{J\pi}_{\alpha lj,\beta l'j'}$	$\lambda^{J\pi}_{\alpha lj,\beta l'j'}$
s$_{1/2}$	$10\frac{1}{2};\ 10\frac{1}{2}$	0.8464	0.9801
p$_{1/2}$	$11\frac{1}{2};\ 11\frac{1}{2}$	73.445	
p$_{3/2}$	$11\frac{3}{2};\ 11\frac{3}{2}$	98.8	
d$_{3/2}$	$12\frac{3}{2};\ 12\frac{3}{2}$	268.9	277.2
d$_{5/2}$	$12\frac{5}{2};\ 12\frac{5}{2}$	2684	2770

potential depth required to reproduce the binding energy for the states $1/2^-$, $1/2^+$, $3/2^-$ and $5/2^+$ are 41.35, 56.90, 28.81 and 56.85 MeV, respectively. For ^{13}N, we use $r_0 = 1.25$ fm, $a = 0.65$ fm and $V_{\rm so} = -10$ MeV (same as in [29]) and the potential depth in this case is 41.65 MeV. We adopted the WS potentials here for convenience, to implement our radiative capture numerical calculations using the code RADCAP [28]. As we have stated before, for bound states, equivalent separable potentials can be found leading basically to the same wavefunctions for these reactions. We thus emphasize that our calculations are consistent with the use of separable potentials for bound and continuum states.

For both of these capture reactions the E1 multipolarity dominates [16, 25, 29]. Hence, we use proper initial angular momenta states in the continuum leading to E1 transitions to the corresponding bound states of each nucleus. For transitions to the ground state of ^{13}C, the proper continuum states have s$_{1/2}$ and d$_{3/2}$ angular momenta, for the 1st e.s. they are p$_{1/2}$ and p$_{3/2}$, for the 2nd e.s. they are s$_{1/2}$, d$_{3/2}$ and d$_{5/2}$ and for the 3rd e.s. it is just the p$_{3/2}$ angular momentum, respectively. Similarly, for E1 transitions to the ground state of ^{13}N, the continuum states taken to be s$_{1/2}$ and d$_{3/2}$.

The calculations of continuum wavefunctions depend upon the phase shifts and hence the scattering matrix, which are obtained by the procedure given in the previous section. As we need only elastic component of S-matrix to calculate the phase shifts, we will only use one single channel, i.e., only the ground state of the target (^{12}C), to calculate the S-matrix. A multi-channel formalism could be taken in order to study the effect of inclusion of more target states on the capture cross sections, provided the fit parameters would be known for all channels under consideration. We use the same set of parameters β, λ as those obtained in [5, 6]. For two cases, discussed later in this section, we employ changes in order to get the best fit with the experimental data. We also generated our own best fit parameters for the p$_{3/2}$ state of ^{13}C by fitting it to the experimental phase shift. In tables 1 and 2, we give the parameters β and λ, respectively, used to obtain the different phase shifts.
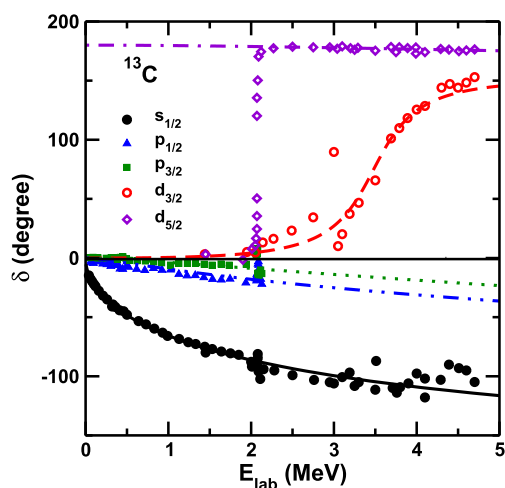
Figure 1. s, p, d phase shifts for n-^{12}C scattering. Solid, dotted–dotted–dashed, dotted, dashed and dotted–dashed lines represent the calculated $s_{1/2}$, $p_{1/2}$, $p_{3/2}$, $d_{3/2}$ and $d_{5/2}$ phase shifts, respectively, whereas filled circles, upper triangles, square boxes, open circles and diamond boxes represent the corresponding experimental data which are taken from [33–35].
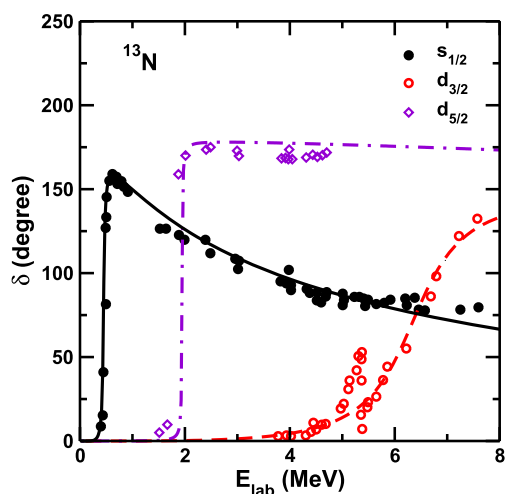

Figure 2. s, d phase shifts for p-^{12}C scattering (solid lines). The symbols and lines are the same as in figure 1. The experimental data are taken from [36–41].

The results of our phase-shift calculations for ^{13}C and ^{13}N are presented in figures 1 and 2, respectively. In both of these figures we plot the phase shifts δ, in degrees, as a function of the laboratory energy E_{lab}. In these figures solid, dotted–dotted–dashed, dotted, dashed and dotted–dashed lines represent the calculated $s_{1/2}$, $p_{1/2}$, $p_{3/2}$, $d_{3/2}$ and $d_{5/2}$ phase shifts, respectively, whereas filled circles, upper triangles, square boxes, open circles and diamond boxes represent the corresponding experimental data taken from [33–35] for n-^{12}C scattering and from [36–41] for p-^{12}C scattering, respectively. For both of these nuclei, we are able to reproduce the results presented in [5]. The calculated phase shifts match well the experimental
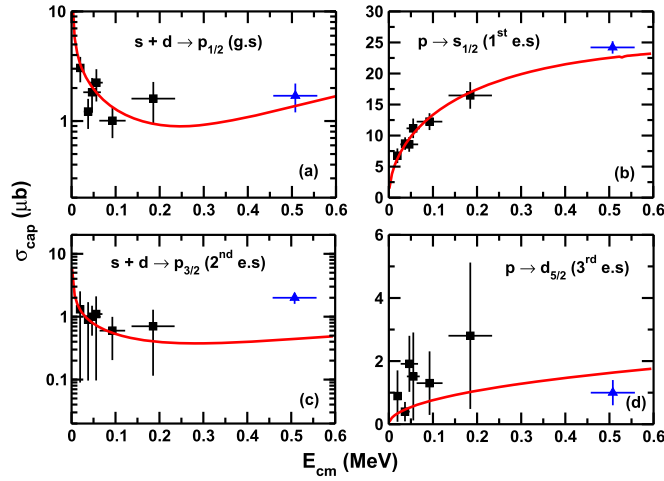
Figure 3. Radiative neutron capture cross sections for capture to the four low-lying states in ^{12}C. Filled Square boxes and filled triangles are the experimental data from [16] and [17], respectively.
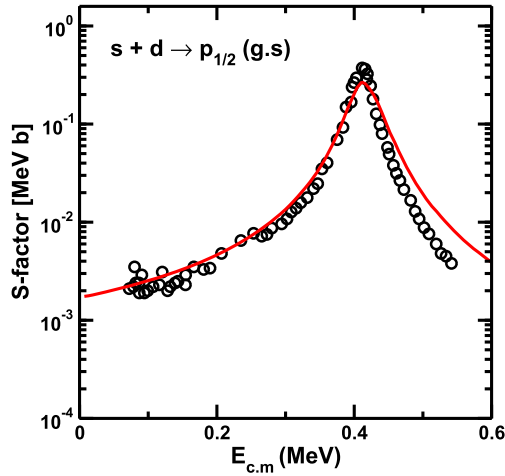
Figure 4. Astrophysical *S*-factor for the ^{12}C$(p, \gamma)^{13}$N reaction. Experimental data are from [25].

data. Furthermore, some narrow resonances for d$_{5/2}$ and d$_{3/2}$ states, both for proton and neutron scattering are found to be of compound nature and can only be explained by considering target excitations to the 2^+ state as in [6]. We also want to point out that for the proton case, the parameter $\beta_{0\frac{1}{2}}$ given in table 1 is slightly corrected to $0.5723\,\mathrm{fm}^{-1}$ to yield a $1/2^+$ resonance at the right position, i.e., at $0.422\,\mathrm{MeV}$ in the c.m., and for a better fit of the experimental phase-shift data, as seen in figure 2. A slight change is also needed for $\beta_{1\frac{1}{2}}$ in the case of ^{13}C, where it is modified from $1.72\,\mathrm{fm}^{-1}$ to $1.76\,\mathrm{fm}^{-1}$ in order to obtain a best fit.

3.2. Capture cross sections

Once the phase shifts have been obtained, we now proceed to calculate the continuum wavefunctions with the asymptotic behavior described in equation (14). We calculate the neutron and proton capture cross sections using equations (1) and (2), as all the quantities are now established.

Given that the continuum wavefunctions are obtained from phase shifts that reproduce experimental data, we expect that our numerical calculations for capture cross sections are more reliable than standard potential models. Figure 3 shows our calculations of neutron capture cross sections (solid line) for capture to different states of ^{13}C compared with respective experimental data. The square boxes in all figures represent data from [16], whereas the upper triangles correspond to experimental data from [17] where the cross sections were measured only at the 0.55 MeV laboratory energy. The spectroscopic factor (C^2S) used for the ground state, the 1st e.s., the 2nd e.s. and the 3rd e.s. are 0.77, 1.0, 0.14, 0.58, respectively. They have been taken from [42], except for the 1st e.s. where C^2S equal to 1.0 in our case. This value explains the data very well. It is clear from the figure that the cross section obtained by this method are in good agreement with the experimental data, especially at low energies.

Figure 4 shows the *S*-factor for proton capture to the ground state of ^{13}N (solid line). The experimental data (open circles) are from [25]. The spectroscopic factor C^2S in this case was chosen to be 0.21, which is quite different than the one used for ground state of ^{13}C. As mentioned earlier, the E1 transition to the ground state of ^{13}N $(1/2^-)$ takes place from s or d continuum wave. The dominant contributions to the cross sections come from the s continuum wave, where there is a resonance at 0.422 MeV, as mentioned earlier. This resonance yields a peak in the cross section which can be seen in the figure 4. Clearly, our calculations again yield a good agreement with the experimental data over the present energy range.

4. Conclusions

We have discussed the utility of quasi-separable potentials to describe nucleon-nucleus scattering and applications to nuclear astrophysics. We have shown how this method can be used to calculate radiative capture cross sections for astrophysical important reactions. As an example, we have considered the case of neutron and proton scattering from ^{12}C, where the scattering phase shifts are used to infer the scattering wavefunctions. The scattering wavefunctions corresponding to the scattering potential parameters determined from phase shifts analysis of the experimental data are used as input to calculate neutron and proton capture cross sections. Our results are in good agreement with the available experimental data in the energy range considered in this work.

This technique can be used to obtain the continuum wavefunctions with a better description of phase-shifts and radiative capture cross sections than the usual potential models. A limitation of using WS or separable potential models (or even any microscopic model) is that, to be consistent, one also needs to reproduce scattering phase shifts or elastic scattering cross sections. While in the WS and separable potential models this is an easy task, just amounting to redefine the potential parameters, in microscopic models it can be a formidable task. The advantage of using separable potentials over WS potential models is the ability to include non-local features. Non-local dependence is of relevance for the treatment of three-body systems, as well as simplifying the calculations enormously. The multi-channel formalism briefly discussed in this paper, can also be used to study

the effects of inclusion of numerous target states on the capture cross sections. The use of a single channel is limited to lower mass nuclei, up to ^{16}O. With the increase of the nuclear mass, the nuclear structure becomes more complicated and one needs to take into consideration the effect of other channels in order to explain the resonances which also become of non-single-particle nature. Applications of this technique to deuteron-induced reactions are in progress.

Acknowledgments

References

[1] Yamaguchi Y 1954 *Phys. Rev.* **95** 1628
[2] Phillips A C 1968 *Nucl. Phys.* A **107** 207
[3] Mongan Thomas R 1968 *Phys. Rev.* **175** 1260
[4] Haidenbauer J and Plessas W 1984 *Phys. Rev. C* **30** 1822
[5] Cattapan G, Pisent G and Vanzani V 1975 *Nucl. Phys.* A **241** 204
[6] Cattapan G, Mglione E, Pisent G and Vanzani V 1978 *Nucl. Phys.* A **296** 263
[7] Miyagawa K and Koike Y 1989 *Prog. Theor. Phys.* **82** 329
[8] Pisent G 1974 *International Centre for Theoretical Physics Report* IC/74/19 Trieste
[9] Alt E O, Mukhamedzhanov A M, Nishonov M M and Sattarov A I 2002 *Phys. Rev. C* **65** 064613
[10] Alt E O, Blokhintsev L D, Mukhamedzhanov A M and Sattarov A I 2007 *Phys. Rev. C* **75** 054003
[11] Wiescher M, Görres J and Schatz H 1999 *J. Phys. G: Nucl. Part. Phys.* **25** R131
[12] Rolfs C E and Rodney W S 1988 *Cauldrons in the Cosmos* (Chicago: Chicago University Press)
[13] Straniero O *et al* 1993 *Astrophys. J.* **413** 324
[14] Mughabghab S F, Lone M A and Robertson B C 1982 *Phys. Rev. C* **26** 2698
[15] Nagai Y, Igashira M, Takeda K, Mukai N, Motoyama S, Uesawa F, Kitazawa H and Fukuda T 1991 *Astrophys. J.* **372** 683
[16] Ohsaki T, Nagai Y, Igashira M, Shima T, Takeda K, Seino S and Irie T 1994 *Astrophys. J.* **422** 912
[17] Kikuchi T, Nagai Y, Suzuki T S, Shima T, Kii T, Igashira M, Mengoni A and Otsuka T 1998 *Phys. Rev. C* **57** 2724
[18] Ho Y-K, Kitazawa H and Igashira M 1991 *Phys. Rev. C* **44** 1148
[19] Mengoni A, Otsuka T and Ishihara M 1995 *Phys. Rev. C* **52** R2334
[20] Lin C J, Zhang H Q, Liu Z H, Wu W Y, Wang F and Ruan M 2003 *Phys. Rev. C* **68** 047601
[21] Baye D 2004 *Phys. Rev. C* **70** 015801
[22] Otsuka T, Ishinhara M, Fukunishi N, Nakamura T and Yokoyama M 1994 *Phys. Rev. C* **49** R2289
[23] Lamb W A S and Hester R E 1957 *Phys. Rev.* **107** 550
[24] Young F C, Armstrong J C and Marion J B 1963 *Nucl. Phys.* **44** 486
[25] Rolfs C and Azuma R E 1974 *Nucl. Phys.* A **227** 291
[26] Burtebaev N *et al* 2008 *Phys. Rev. C* **78** 035802
[27] Bertulani C A and Kajino T 2016 *Prog. Part. Nucl. Phys.* **89** 56
[28] Bertulani C A 2003 *Comput. Phys. Commun.* **156** 123
[29] Huang J T, Bertulani C A and Guimarães V 2010 *At. Data Nucl. Data Tables* **96** 824
[30] Mukhamedzhanov A M, Shubhchintak and Bertulani C A 2016 *Phys. Rev. C* **93** 045805
[31] Lawson R D 1980 *Theory of the Nuclear Shell Model* (Oxford: Clarendon Press)
[32] Kruppa A T and Papp Z 1985 *Comput. Phys. Commun.* **36** 59
[33] Wills J E Jr, Bair J K, Cohn H O and Willard H B 1958 *Phys. Rev.* **109** 891
[34] Lister D and Sayres A 1966 *Phys. Rev.* **143** 745
[35] Pisent G and Saruis A M 1963 *Nuovo Cimento* **28** 600

J. Phys. G: Nucl. Part. Phys. **43** (2016) 125203

Shubhchintak *et al*

[36] Reich C W, Phillips G C and Russel J L 1956 *Phys. Rev.* **104** 143
[37] Moss S J and Haeberli W 1965 *Nucl. Phys.* **72** 417
[38] Jackson H L and Galonsky A I 1953 *Phys. Rev.* **89** 370
[39] Bernstein E M and Terrel G E 1968 *Phys. Rev.* **173** 937
[40] Trachslin W and Brown L 1967 *Nucl. Phys.* A **101** 273
[41] Drigo L, Manduchi C, Nardelli G, Russo-Manduchi M T and Zannoni G 1964 *Phys. Rev.* **136** B1662
[42] Ohnuma H *et al* 1985 *Nucl. Phys.* A **448** 205